

Title	Weld Cold Cracking in HAZ of Engineering Carbon and Low Alloy Steel (Report III) : Effect of Chemical Composition on Cold Cracking Susceptibility of Quenching Crack Type(Materials, Metallurgy & Weldability)
Author(s)	Matsuda, Fukuhisa; Nakagawa, Hiroji; Park, Hwa Soon
Citation	Transactions of JWRI. 1987, 16(1), p. 115-122
Version Type	VoR
URL	https://doi.org/10.18910/9189
rights	
Note	

Osaka University Knowledge Archive : OUKA

<https://ir.library.osaka-u.ac.jp/>

Osaka University

Weld Cold Cracking in HAZ of Engineering Carbon and Low Alloy Steel (Report III)[†]

— Effect of Chemical Composition on Cold Cracking Susceptibility of Quenching Crack Type —

Fukuhisa MATSUDA*, Hiroji NAKAGAWA** and Hwa Soon PARK***

Abstract

For evaluation of crack susceptibility of medium, high carbon low alloy steels to quenching crack type cold cracking in HAZ of welds, the effect of hardness and chemical compositions on fracture stress was studied by linear multiple regression analysis, where the fracture stress was measured by the simulated cold cracking test under the cooling condition causing no bainite and ferrite.

The fracture stress has a tendency to decrease with an increase of carbon content or hardness. Phosphorus is very harmful because of decreasing fracture stress and increasing inter granular fracture. The regression equation for fracture stress giving a good correlation with the measured fracture stress is obtained by use of hardness, phosphorus, nitrogen and oxygen.

KEY WORDS: (Low Alloy Steels) (Carbon Steels) (Tool Steels) (Cold Cracking) (Simulating) (Composition)

1. Introduction

In the previous paper¹⁾, it was shown that the cracking stress in the RRC test for medium, high carbon low alloy steels susceptible to cold cracking of quenching crack type can be evaluated by the fracture stress obtained by the simulated cold cracking test. Now, it is interesting to study the effect of chemical compositions on the susceptibility to this type of cold cracking, that is, on the fracture stress by the simulated cold cracking test.

Therefore, in this report, the effect was studied by means of regression analysis on the fracture stress of different steels, which were thought to be susceptible to this type of cold cracking and were easily obtainable as commercial steels, though laboratorial steels were partly included.

2. Materials Used and Experimental Procedures

2.1 Materials used

Table 1 shows the chemical compositions of materials used, which are classified into a kind of machine structural medium carbon low alloy steel (SCr440, SCM440, SNCM439, SCr445, SCM445 and SNCM447), plain carbon tool steel (SK6, SK5 and SK3) and high carbon

chromium bearing steel (SUSJ2).

The steels except for SNCM447 (2) to (5) are commercial steels. The steels SNCM447 (2) to (5) are laboratorial steels made by vacuum melting with high frequency induction heating, and contain two levels of phosphorus and sulphur, that is, about 0.03% and 0.001%. The detail of these laboratorial steels will be explained in the following paper²⁾.

2.2 Experimental procedures

The simulated cold cracking test was established in the previous report¹⁾ was used, which was in notch tensile test during cooling of simulated weld thermal cycle. The shape and size of the simulated cold cracking test specimen is shown in Fig. 1. The cooling stage of the thermal cycle shown in Fig. 2 was programmed so as to agree with that measured in Tekken test for 25 mm thickness steel with GTA welding under the condition of welding current of 300A, arc voltage of 19V and welding speed of 2 mm/sec. Consequently, cooling time from 1073 to 773K, $\Delta t_{1073-773K}$, was about 3.5 sec. Based on the result in the previous report¹⁾, the peak temperature with holding time of 6 sec was set to the liquation temperatures of grain boundary in each steel. The peak temperature causing grain boundary liquation are summarized in Table 2. Examples of the microstructure showing grain boundary

[†] Received on May 6, 1987

* Professor

** Research Instructor

*** Graduate Student of Osaka Univ.

Transactions of JWRI is published by Welding Research Institute of Osaka University, Ibaraki, Osaka 567, Japan

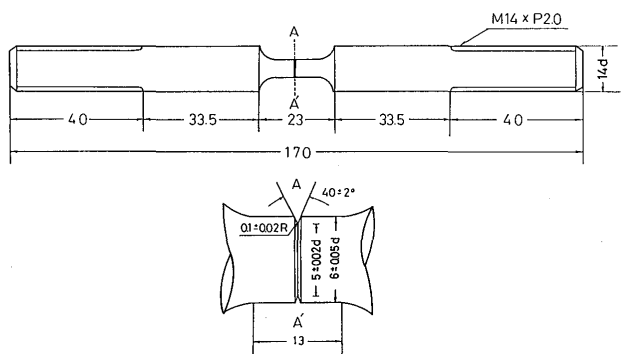
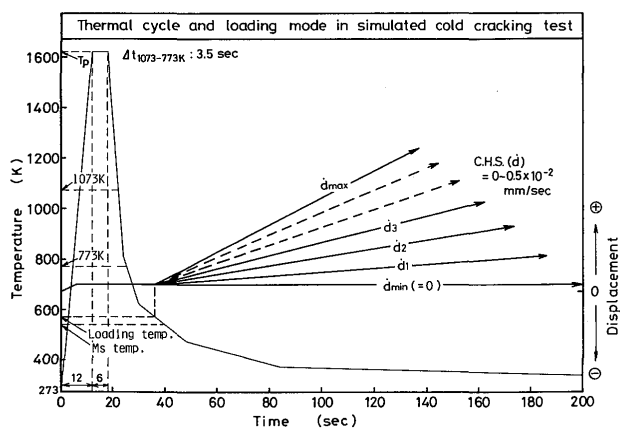
Table 1 Chemical compositions of materials used

Material*	Chemical composition (wt.%)									
	C	Si	Mn	P	S	Ni	Cr	Mo	N	O
SCr440	0.40	0.29	0.76	0.025	0.012	0.07	1.09	0.02	0.0120	0.004
SCM440	0.40	0.27	0.71	0.018	0.028	0.08	1.05	0.16	0.0100	0.001
SNCM439	0.39	0.28	0.73	0.012	0.007	1.72	0.69	0.17	0.0094	0.003
SCr445	0.49	0.26	0.78	0.020	0.024	0.07	1.03	0.02	0.0067	0.001
SCM445	0.45	0.24	0.78	0.017	0.018	0.07	1.07	0.15	0.0140	0.001
SNCM447(1)	0.44	0.22	0.69	0.015	0.007	1.68	0.71	0.16	0.0080	0.002
SNCM447(2)	0.48	0.24	0.75	0.001	0.001	1.72	0.83	0.22	0.0011	0.004
SNCM447(3)	0.47	0.26	0.76	0.034	0.001	1.82	0.80	0.24	0.0006	0.001
SNCM447(4)	0.48	0.26	0.75	0.002	0.030	1.80	0.80	0.24	0.0007	0.001
SNCM447(5)	0.50	0.25	0.76	0.031	0.032	1.80	0.79	0.24	0.0006	0.002
SK6**	0.72	0.22	0.75	0.025	0.023	0.07	0.22	0.01	0.0096	0.002
SK5	0.89	0.24	0.29	0.022	0.020	0.04	0.12	-	0.0043	0.001
SK3**	1.05	0.33	0.98	0.020	0.018	0.05	0.47	-	0.0130	0.001
SUJ2	0.96	0.26	0.46	0.015	0.009	0.05	1.46	0.01	0.0073	0.001

† Sn contents ranged from 0.001 to 0.023 wt.%

* Designations follow JIS

** Mn and Cr content are a little higher than that specified in JIS

**Fig. 1** Configuration of simulated cold cracking test specimen.**Fig. 2** Thermal cycle and loading mode in simulated cold cracking test

liquation near notch, which were etched with aqueous solution of saturated picric acid including wetting agent,

Table 2 Summary of peak temperature causing grain boundary liquation

Material	Tp(K)	Material	Tp(K)	Material	Tp(K)
SCr440	1633	SNCM447(1)	1628	SK6	1558
SCM440	1638	SNCM447(2)	1628	SK5	1548
SNCM439	1638	SNCM447(3)	1623	SK3	1543
SCr445	1628	SNCM447(4)	1621	SUJ2	1548
SCM445	1628	SNCM447(5)	1619		

are shown in Fig. 3.

The loading mode used was also the same as that of the previous report¹⁾ as shown in Fig. 2, that is, the displacement of chuck was generally fixed from the start of cooling to the temperature just above Ms point and then was increased under different cross-head speeds between 0 to 0.005 mm/sec. This range of C.H.S. was selected so that the fracture might occur in 323 to 373K, because it was shown in the RRC test³⁾ that this type of cold cracking generally occurs about this temperature range.

2.3 Measurement of area fraction of intergranular fracture surface

Fracture surfaces were observed by scanning electron microscope (SEM) to determine fracture surface. The area fraction of intergranular fracture surface was measured by point counting method using 5 mm square mesh on the microfractographs of magnification from 50X to 200X in each case.

3. Experimental Results and Discussions

The microstructure near notch of all the steels after testing given martensite (and partial retained austenite), and the examples etched with 2% Nital + 2% Picral are shown in Fig. 4.

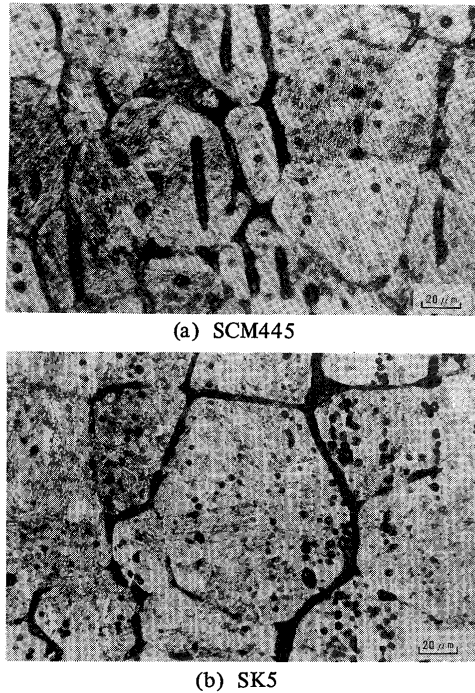


Fig. 3 Microstructure showing grain boundary liquation near notch, etched with aqueous solution of saturated picric acid including wetting agent

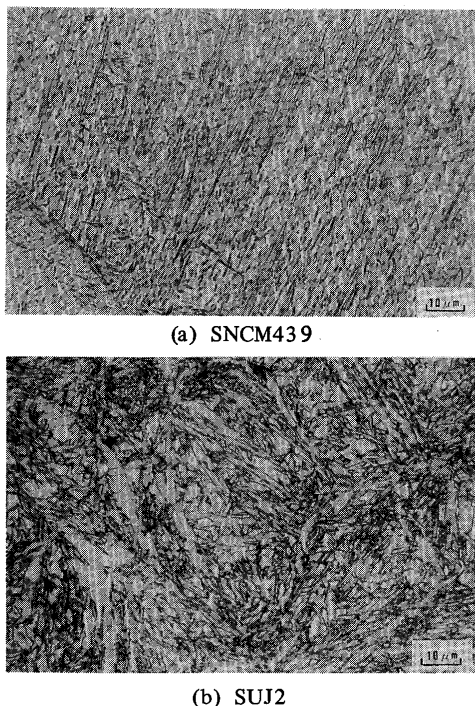


Fig. 4 Microstructure near notch under the cooling condition of $\Delta t_{1073-773K}$; 3.5 sec, etched with 2% Nital + 2% Picral

Figure 5 shows the example of the relationship between temperature and fracture stress in SNCM 447 and SK6. The fracture stress in SNCM447 give a tendency to decrease slightly with decreasing in temperature near 400K and were nearly constant at about 460 MPa below 370K. In SK6, the fracture stresses are lower than that of SNCM447 and nearly constant at about 250 MPa in over-all temperature.

The mean fracture stress in 323 to 373K of all materials are listed in sequence of carbon content in Fig. 6, with hardness near notch measured by loading of 9.8 N. The fracture stresses ranged from about 700 MPa with Hv of about 650 to about 200 MPa with Hv of about 850.

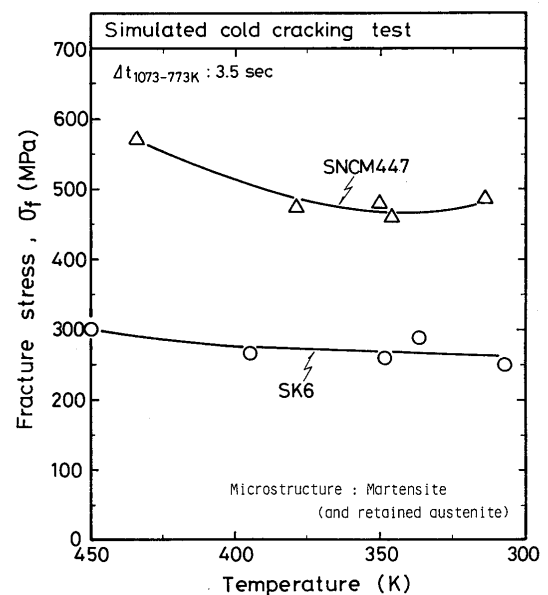
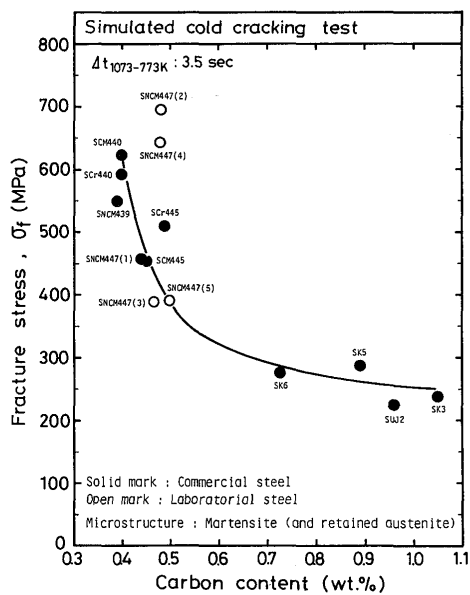


Fig. 5 Relationship between temperature and fracture stress in SNCM439 and SK6

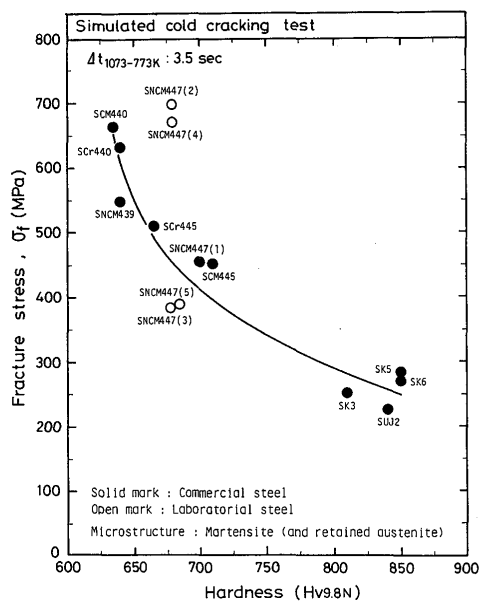
Simulated cold cracking test		$\Delta t_{1073-773K}$: 3.5 sec									
Carbon (wt%)	Material	100	200	300	400	500	600	700	800		
0.40	SCr440										(640)
	SCM440										(635)
	SNCM439										(640)
0.45	SCr440										(665)
	SCM440										(710)
0.47	SNCM447 (1)										(700)
	" (2)										(685)
	" (3)										(685)
0.50	" (4)										(690)
	" (5)										(690)
0.72	SK6										(850)
0.89	SK5										(850)
0.96	SUJ 2										(840)
1.05	SK3										(810)

Fig. 6 Summary of mean fracture stress in temperature range of 323 to 373K

Except for SNCM447 (2) and (4) which contain very low phosphorus, the fracture stress has a tendency to decrease with an increase in carbon content, or with an increase in hardness. These tendencies are given in Fig. 7 (a) and (b), where solid marks mean commercial steels and open marks do laboratorial ones. It is noteworthy that laboratorial SNCM447 (3) and (5) containing much phosphorus similar to those in commercial steels nearly locate on the curve showing the correlation between fracture stress vs. carbon content or hardness. On the other hand, the laboratorial SNCM447 (2) and (4) containing little phosphorus deviate considerably from the curve. These mean that the susceptibility to this type cold cracking is mainly related to carbon content or to hardness in com-



(a)



(b)

Fig. 7 Effect of (a) carbon content, (b) hardness on fracture stress

mercial steels, and that phosphorus and sulphur have a definite and little effect, respectively. The detailed effects of phosphorus and sulphur will be discussed in the following paper²⁾.

One of the characteristics of this type cold cracking is marked occurrence of intergranular fracture surface as shown in Fig. 8, and fracture stress vs. its area fraction is shown in Fig. 9. The materials except for SNCM447 (2) and (4) containing very low phosphorus give area fraction higher than about 75%, and the fracture stress has a tendency to decrease with an increase in intergranular area fraction. The area fraction of SNCM447 (2) and (4) is very little compared with the other materials, and this suggests that phosphorus has an effect to embrittle grain boundaries. By the way, it is noticeable the gradient of broken line located in the intergranular area fraction less than about 75% is smoother than that of solid line located in the area fraction more than about 75%. The reason why the gradient of the broken line is smoother is considered to be not due to an peculiarity of SNCM447 (2) and (4),

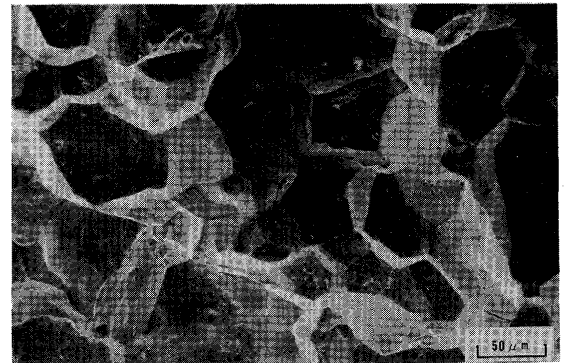


Fig. 8 Typical SEM microfractograph of intergranular fracture surface in SCM445

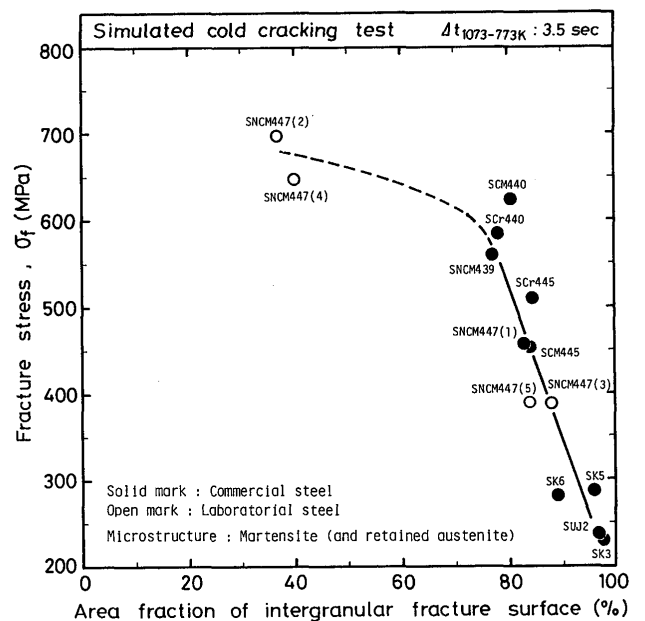


Fig. 9 Relationship between fracture stress and area fraction of intergranular fracture surface

but due to the well known fact that quenched martensite itself of the materials causing transgranular fracture has not so high fracture toughness or fracture stress.

Figure 10 shows the relationship between hardness and the area fraction of intergranular fracture surface. The area fraction of intergranular fracture surface has a tendency to increase with increasing in hardness in commercial steels. However, the area fraction of intergranular fracture surface of SNCM447 (2) and (4) containing very low phosphorus deviated considerably from the tendency.

The regression analysis for the area fraction of intergranular fracture surface was done by use of hardness and phosphorus. Equation (1) shows the effect of hardness and phosphorus on the area fraction of intergranular fracture surface, and the relationship between the area fraction of intergranular fracture surface calculated by Eq. (1) (IG fraction_{cal}) and that measured (IG fraction_{exp}) is shown in Fig. 11.

$$\text{IG fraction}_{\text{cal}} [\%] = 0.920 \cdot \text{Hv} + 1350 \cdot [\text{wt.\%P}] - 11.9 \quad (1)$$

, where the coherency which is represented by square of correlation coefficient is 71.4%. Thus the effect of phosphorus on intergranular fracture was also confirmed by the regression analysis even though the coherency was somewhat low.

Thus, according to the results shown in Figs. 9 to 11, the decreasing of fracture stress is accompanied with an increase of the area fraction of intergranular fracture sur-

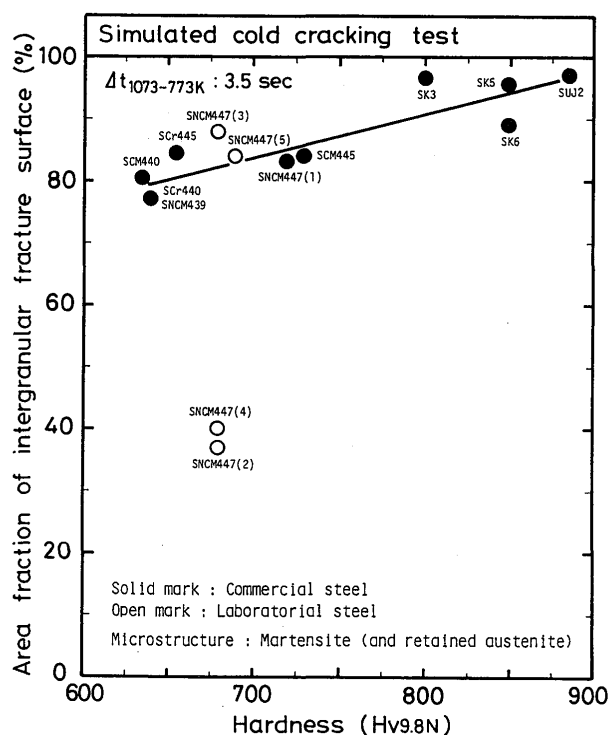


Fig. 10 Relationship between hardness and area fraction of intergranular fracture surface

face, and the intergranular area fraction is related with not only hardness but also phosphorus content.

In the following, the fracture stress mentioned in the above was treated by means of linear multiple regression analysis for the purpose of practicality in welding design and so on.

The regression equation between carbon and fracture stress is given in Eq. (2), and relationship between $\sigma_{f \text{ cal}}$ and $\sigma_{f \text{ exp}}$ is shown in Fig. 12 (a), where $\sigma_{f \text{ cal}}$ and $\sigma_{f \text{ exp}}$ are the fracture stress calculated by the regression equation and that obtained by experiments, respectively.

$$\sigma_{f \text{ cal}} [\text{MPa}] = -568 \cdot [\text{wt.\%C}] + 783 \quad (2)$$

In this case, coherency R^2 was 64.4%, and thus the correlation is not satisfactory.

The regression equation between hardness and fracture stress is given in Eq. (3), and the relationship between $\sigma_{f \text{ cal}}$ and $\sigma_{f \text{ exp}}$ is shown in Fig. 12 (b).

$$\sigma_{f \text{ cal}} [\text{MPa}] = -1.55 \cdot \text{Hv} + 1570 \quad (3)$$

, where Hv is the mean Vickers hardness near notch with loading of 9.8 N. In this case, coherency R^2 was 69.9%, and thus the correlation is not also satisfactory even though it is somewhat high compared with that of carbon.

The results of the regression analysis used for only commercial steels are shown in Eqs. (4) and (5), and Fig. 13 (a) and (b).

$$\sigma_{f \text{ cal}} [\text{MPa}] = -540 \cdot [\text{wt.\%C}] + 756 \quad (4)$$

$$\sigma_{f \text{ cal}} [\text{MPa}] = -1.48 \cdot \text{Hv} + 1520 \quad (5)$$

In either case, coherencies are fairly high compared with

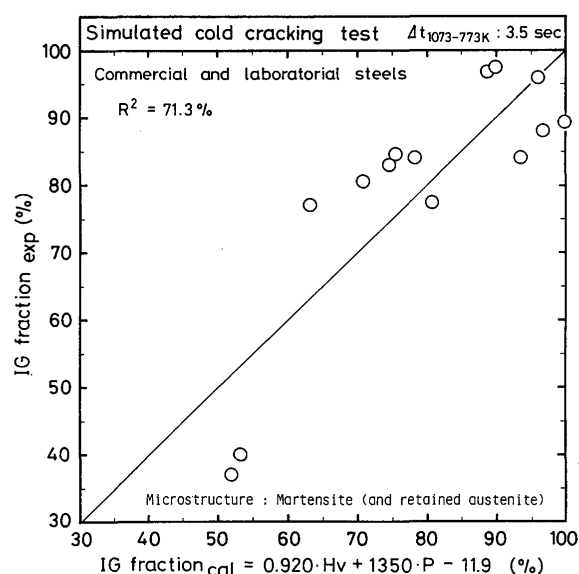


Fig. 11 Comparison of area fraction of intergranular fracture surface measured (IG fraction_{exp}) and that calculated (IG fraction_{cal}) by Eq. (1) taking account of hardness and phosphorus.

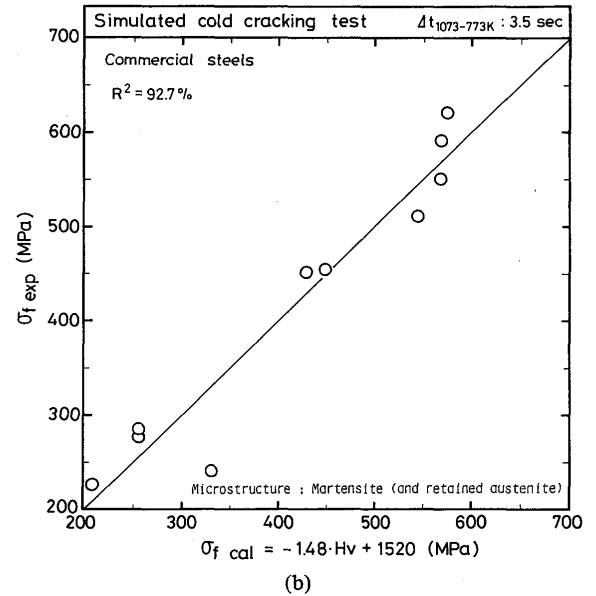
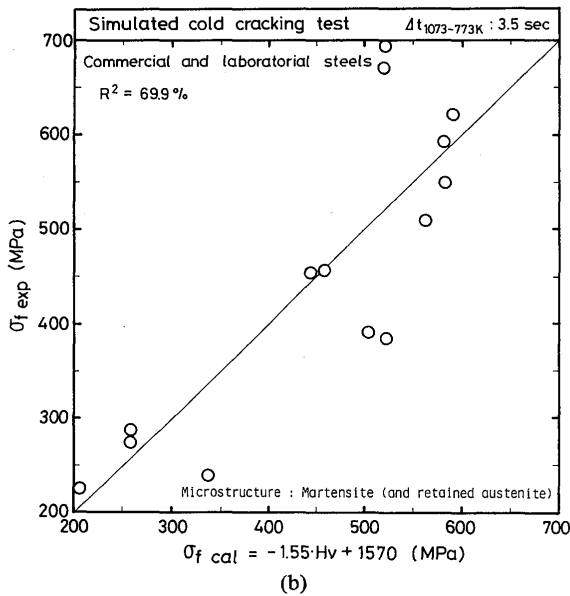
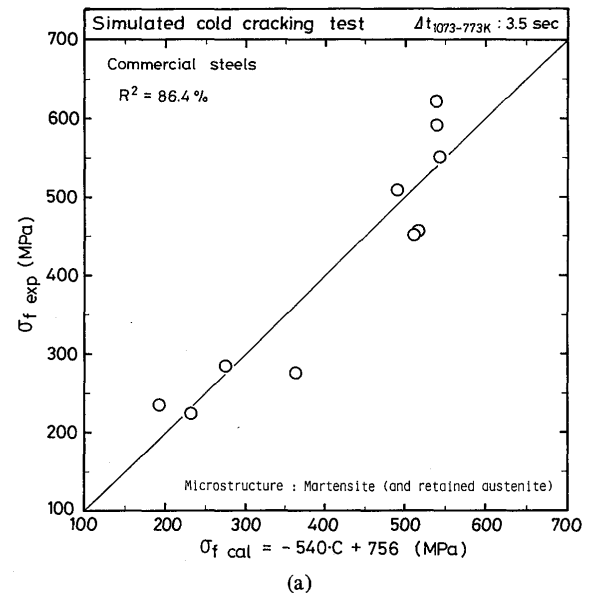
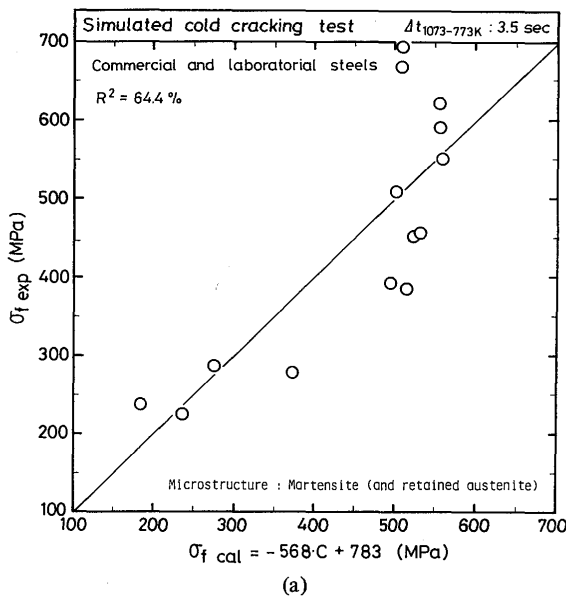


Fig. 12 Comparison of fracture stress ($\sigma_{f \text{ exp}}$) and that calculated ($\sigma_{f \text{ cal}}$) by (a) Eq. (2), (b) Eq. (3) taking account of (a) carbon content, (b) hardness.

Fig. 13 Comparison of fracture stress measured and that calculated by (a) Eq. (4), (b) Eq. (5) taking account of (a) carbon content, (b) hardness in case of only commercial steels.

those in Fig. 12 (a) and (b) used for all of the steels. Therefore, in the case of commercial steels, it was thought that crack susceptibility to this type cold cracking may be evaluated by the use of carbon content or hardness.

Now, the effect of phosphorus was taken account of in addition to hardness, and the regression equation is shown in Eq. (6) and the relationship between $\sigma_{f \text{ cal}}$ and $\sigma_{f \text{ exp}}$ is shown in Fig. 14.

$$\sigma_{f \text{ cal}} [\text{MPa}] = -1.46 \cdot H_v - 7840 \cdot [\text{wt.\%P}] + 1650 \quad (6)$$

In this case, coherency R^2 of 90.7% showed good correlation. The regression coefficient of phosphorus in Eq. (6) gives large negative value. Thus it was confirmed that

phosphorus was important factor to increase crack susceptibility of this type cold cracking.

Furthermore, the effect of nitrogen and oxygen which are well known to promote intergranular fracture in various type fracture of iron and steels was taken account of in addition to hardness and phosphorus. The regression equation is shown in Eq. (7) and the relationship between $\sigma_{f \text{ cal}}$ and $\sigma_{f \text{ exp}}$ is shown in Fig. 15.

$$\sigma_{f \text{ cal}} [\text{MPa}] = -1.37 \cdot H_v - 7470 \cdot [\text{wt.\%P}] - 2180 \cdot [\text{wt.\%N}] + 14700 \cdot [\text{wt.\%O}] + 1570 \quad (7)$$

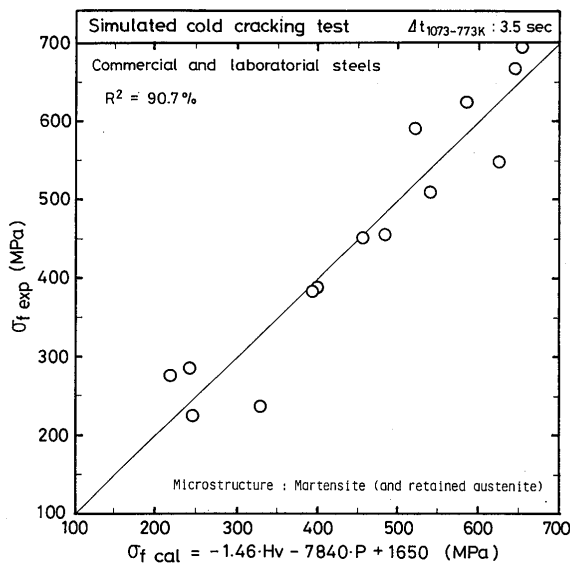


Fig. 14 Comparison of fracture stress measured and that calculated by Eq. (6) taking account of hardness and phosphorus.

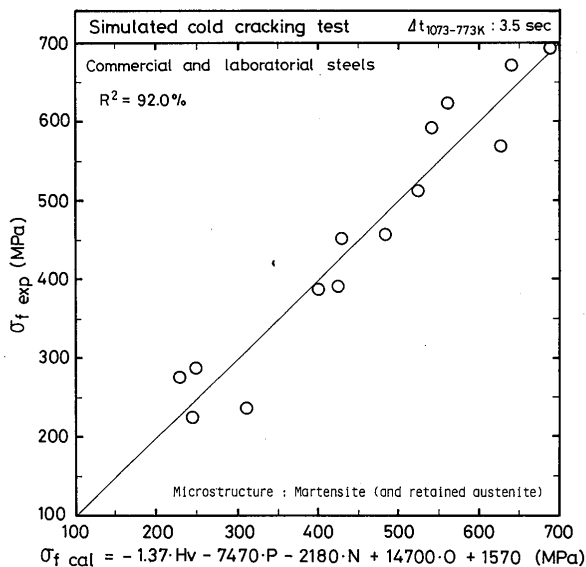


Fig. 15 Comparison of fracture stress measured and that calculated by Eq. (7) taking account of hardness, phosphorus, nitrogen and oxygen

In the case, coherency R^2 was 92.0%, thus the relation showed good correlation. According to the regression Eq. (7), the regression coefficient of nitrogen and oxygen are negative and positive, respectively. This means that nitrogen has an effect to lower the fracture stress similar to phosphorus. The regression coefficient of nitrogen is, however, one third times as large as that of phosphorus. It seems that oxygen has an effect to improve fracture stress effectively. However, it should not be expected that oxygen is available to improve the crack susceptibility, because oxygen content should be lowered from the viewpoint of the cleanliness and the fracture toughness etc. of

steels, and because the improvement of $\sigma_{f\text{ cal}}$ by Eq. (7) in the range of oxygen content shown in Table 1 is only about 40 MPa. Similarly, the deterioration of $\sigma_{f\text{ cal}}$ by eq. (7) in the range of the nitrogen content in Table 1 is only about 30 MPa. Therefore, reduction of phosphorus content is most available to lower the crack susceptibility.

It is well known⁴⁻⁶⁾ that stannum promotes temper embrittlement showing intergranular fracture. According to the result of regression analysis, however, the regression coefficient of stannum was little.

4. Conclusions

In order to evaluate the effect of hardness and elements on the susceptibility to cold cracking of quenching crack type, the fracture stress measured with the simulated cold cracking test for fourteen kinds of steels was studied by means of regression analysis. Main conclusions obtained are as follows:

- (1) The fracture stress has a tendency to decrease with an increase of carbon content or hardness. Especially, this tendency was clear in commercial steels. However, improving of fracture stress by reducing phosphorus was noticeable.
- (2) The fracture stress has a good correlation with the area fraction of intergranular fracture surface. The area fraction was correlated with not only hardness but also phosphorus content.
- (3) Regression analysis was done for different kinds of variables, namely for only carbon, only hardness, hardness + phosphorus and hardness + phosphorus + nitrogen + oxygen, and the last gave the best correlation. That is,

$$\sigma_{f\text{ cal}} = -1.37 \cdot \text{Hv} - 7470 \cdot [\text{wt.\%P}] - 2180 \cdot [\text{wt.\%N}] + 14700 \cdot [\text{wt.\%O}] + 1570$$

where, coherency R^2 was 92.0%. The applicable range of the equation is as follows: Hv; 635–850, P; 0.001–0.034(%), N; 0.0006–0.0140(%), O; 0.001–0.004(%), where Hv is the mean Vickers hardness by loading of 9.8N and microstructure is martensite (and partial retained austenite) under the cooling condition of $\Delta t_{1073-773\text{K}}$ of about 3.5 sec. According to this equation, phosphorus and nitrogen have harmful effect and oxygen has a beneficial effect. However, considering their contents in commercial steels, the effect of phosphorus is the most, and the effects of nitrogen and oxygen are nearly negligible. Therefore, reduction of phosphorus content is useful to improve the crack susceptibility.

Acknowledgement

The authors would like to thank Sumitomo Metal Industries, LTD. for the offering of a part of materials used, and Mr. M. Inada, formerly the student of Kinki Univ., for his cooperation in this experiment.

References

- 1) F. Matsuda, H. Nakagawa and H. S. Park: Trans. JWRI, 15-2 (1986), 143-146.
- 2) F. Matsuda, H. Nakagawa and H. S. Park: *ibid*, to be published.
- 3) F. Matsuda, H. Nakagawa, H. S. Park, T. Murakawa and M. Yamaguchi: *ibid*, 15-2 (1986), 135-141.
- 4) I. Olefjord: Int. Met. Rev., No. 4 (1978), 149-163.
- 5) T. Takamatsu, Y. Otoguro, K. Shiotsuka and K. Hashimoto: JISI of Japan, 67-1 (1981), 178-187 (in Japanese).
- 6) K. Hashimoto, Y. Otoguro, T. Saito, T. Takada and T. Kikutaka: *ibid.*, 72-15 (1986), 2093-2101 (in Japanese).